

An Integrated Online System for Monitoring Metals in Surface Water via Automated Sample Preparation-Solution Cathode Glow Discharge-Optical Emission Spectrometry (ASP-SCGD-OES)

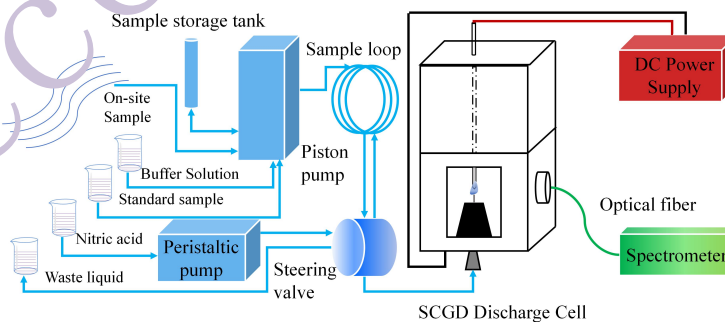
Peichao Zheng*, Xuanyu Luo, Jinmei Wang*, Tao Hu, Junhao Xiang, Biyong Zhang, Jialong Li, and Yan Liu

Chongqing Municipal Level Key Laboratory of Photoelectronic Information Sensing and Transmitting Technology, School of Electronic Science and Engineering, Chongqing University of Posts and Telecommunications, Chongqing 400065, P. R. China

Received: January 12, 2026; Revised: May 30, 2026; Accepted: June 01, 2026; Available online: June 01, 2026.

DOI: 10.46770/AS.2026.0003

ABSTRACT: Long-term online monitoring of metals in surface water is essential to protect water resources. Herein, a novel, integrated analytical system encompassing an automatic sample preparation system and solution cathode glow discharge-optical emission spectroscopy (SCGD-OES) for continuous and real-time detection of metals in rivers is presented. A piston pump integrated with a switching valve in the SCGD-OES system enables on-site preparation of water samples and controlled injection of a standard solution with a gradient concentration or environmental samples directly into the SCGD unit. Corresponding hardware and software platforms were developed to support automated operation. Under laboratory conditions, the achieved limits of detection (LODs) for typical metal ions, e.g., Na, K, Ca, and Mg, are comparable to those of conventional SCGD setups. The evaluation of the SCGD system using certified reference materials (CRMs) for water samples demonstrated satisfactory performance for elemental quantitative analysis, with relative errors of 4.1%, 1.9%, 4.0% and 4.5% for the four elements Na, K, Ca and Mg respectively. Furthermore, a seven-day field deployment of the SCGD system at a riverine site confirmed its accuracy and stability, with a relative error of less than 5.7% relative to reference ICP-OES measurements. These results validate the ability of the SCGD system to provide reliable and continuous online monitoring of metals in surface water.



INTRODUCTION

The monitoring of free metal species in surface water is critical for assessing water quality, safeguarding public health, and managing environmental resources.¹ Elevated concentrations of certain metals, such as Pb, Cd, and Ga, pose a significant risk to human health, requiring active monitoring of their levels in potable water.^{2,3} Conversely, quantifying Na, K, Ca, and Mg in environmental water bodies is valuable for geological prospecting and hydrological studies.⁴ Traditional quantitative analyses of aqueous metal species rely on well-established spectrometric techniques,

including inductively coupled plasma-mass spectrometry (ICP-MS), inductively coupled plasma-optical emission spectroscopy (ICP-OES), flame atomic absorption spectrometry (F-AAS), atomic fluorescence spectroscopy (AFS), and X-ray fluorescence spectroscopy (XRF).^{5,6} However, in spite of high sensitivity and selectivity and superior performance, devices based on these spectroscopic technologies currently are not suitable for real-time, on-site, multi-element monitoring. For example, Although significant breakthroughs have been made in recent years in

miniaturising ICP-MS/OES equipment, maintaining a stable capacitively coupled plasma still requires the use of high-pressure argon cylinders and high-power power supplies, which means that the cost of on-site deployment remains high⁷, while F-AAS, although widely used, is susceptible to numerous chemical and spectral interferences.⁵ Consequently, a significant gap exists between the possibilities offered by conventional spectroscopic laboratory analyses and the growing demand for on-site, real-time, multi-element detection in surface water.

Solution cathode glow discharge-Optical emission spectroscopy (SCGD-OES) has recently emerged as a compelling alternative for liquid sample analysis. SCGD-OES utilizes a solution as a flowing cathode, sustaining a stable microplasma against a metal anode to atomize and excite analyte atoms.⁸ SCGD-OES, initially termed electrolyte-cathode discharge (ELCAD)⁹, has been innovated since its inception, including the geometrical optimization of the discharge cell¹⁰, the introduction of low-molecular-weight organic compounds^{11, 12} and surfactants into solution^{13, 14}, and the application of advanced data processing techniques such as neural networks¹⁵, to enhance its analytical performance. The simplicity, operational robustness, straightforward solution-based sampling, low cost, and minimal sample consumption required for SCGD-OES made this technique an excellent means for analyzing diverse sample, e.g., surface water¹⁶⁻¹⁸, food^{19, 20}, solid materials^{4, 21}, and biological fluids^{22, 23}, and particularly attractive for field deployment. Following these advantages, Zu et al. developed a portable SCGD instrument for thallium detection in water²⁴, Peng et al. demonstrated a battery-operated, high-throughput portable SCGD device²⁵, while Hu et al. integrated a multifunction sample injection system to enhance the operational flexibility of SCGD.²⁶ The introduction of these machines has greatly expanded the applications of SCGD.

In recent years, portable and miniaturized spectrometers based on microplasma technology have demonstrated immense potential for application in on-site monitoring and point-of-care testing due to their compact size and low power consumption. For example, by combining low-cost micro-ultrasonic nebulisation with atmospheric pressure air-assisted discharge (APAD) technology, researchers have successfully developed a carrier-gas-free portable system and applied it to the rapid analysis of serum samples²⁷. This clearly demonstrates that instrument miniaturisation is a key trend in the practical application of microplasma technology.

However, the direct application of SCGD technology to long-term online or portable in-situ monitoring of natural water bodies still faces significant engineering and methodological challenges. Firstly, the microplasma volume in SCGD is extremely small, making it highly susceptible to interference from fluid pulsations and solvent quenching effects. To maintain plasma discharge

stability and enhance analytical sensitivity, conventional systems typically require the introduction of complex peripheral sampling or dewatering devices, such as membrane desolvation systems to pre-strip water molecules²⁸. Whilst this design improves performance, it significantly increases instrument fragility and the complexity of flow path control, making it difficult to adapt to harsh field conditions involving continuous sampling. Secondly, current SCGD systems remain highly reliant on offline manual pretreatment during field applications (such as the manual addition of strong acids to adjust solution conductivity). Consequently, despite its many advantages, a critical limitation of SCGD systems, i.e., a lack of integrated, automated sample preparation, persists, and the reliance on manual pre-treatment procedures hinders completely autonomous, long-term online monitoring.

Herein, an Automated Sample Preparation SCGD-OES (ASP-SCGD-OES) system was developed as a fully integrated analytical platform that automates the entire workflow, from standard curve generation and sample pre-treatment to spectral acquisition and quantitative analysis, for detecting multiple metal elements in surface water. The core innovation of ASP-SCGD-OES is a programmable fluidic subsystem that performs all necessary on-site preparation and injection steps. The rationale behind the system's design was explained, with a comprehensive analytical validation, demonstrating the excellent suitability of ASP-SCGD-OES for the autonomous monitoring of metals in natural waters via laboratory and extended field testing.

EXPERIMENTAL

Overall System Architecture. The ASP-SCGD-OES system was conceived as a fully integrated analytical system for autonomous, sustained field deployment. The hardware and software components are designed around three functionally distinct yet interconnected subsystems, as illustrated in Fig. 1: (1) the sample injection and preparation subsystem automates handling, preparation, and introduction of standard solutions and real samples; (2) the discharge and detection subsystem generates plasma and acquires atomic emission spectra; finally, (3) the control and analysis subsystem orchestrates all system operations and performs real-time data processing.

The entire monitoring procedure is managed by the control and analysis subsystem. A centralized Industry PC (IPC) serves as the system controller that communicates with a microcontroller board via a standardized protocol (e.g., RS485) to govern lower-level hardware components within the sample injection and preparation subsystem and the discharge and detection subsystem. Concurrently, the IPC runs custom-developed software for real-time spectral acquisition, processing, and quantitative analysis. Fig. 2 depicts the functional hierarchy and data flow between these subsystems.

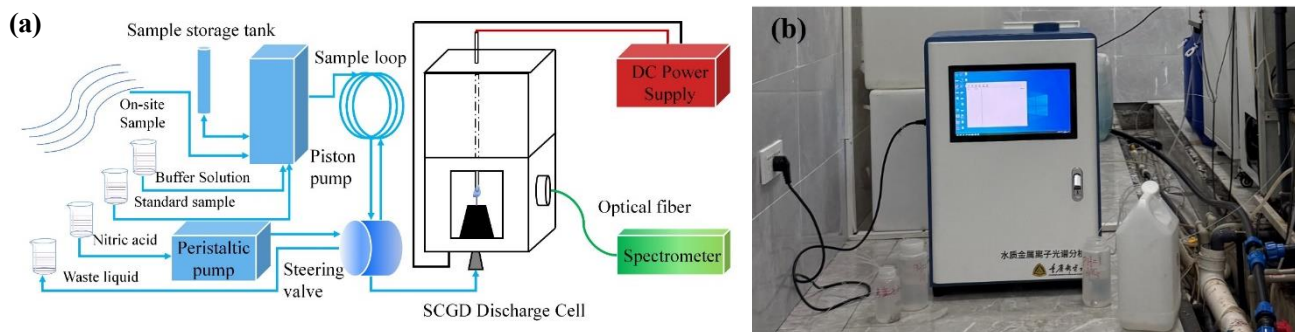


Fig. 1 (a) Schematic diagram of the overall system's design. (b) A photograph of the internal system.

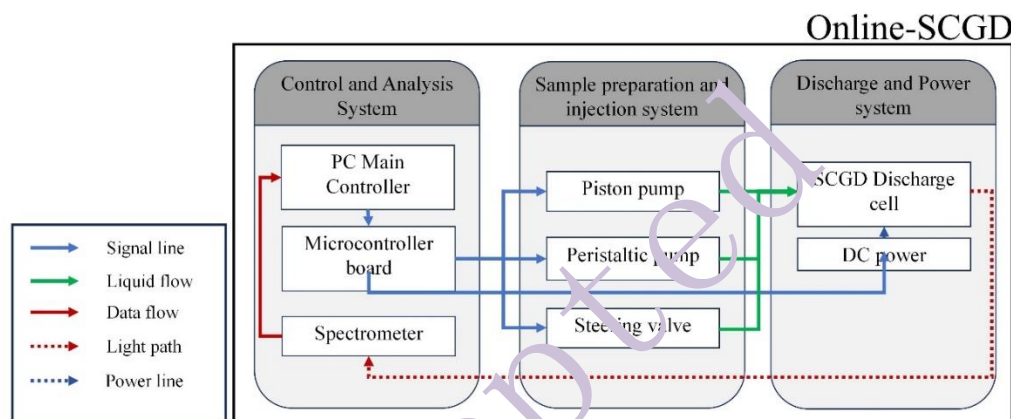


Fig. 2 (a) Schematic diagram of the overall system's design. (b) A photograph of the internal system.

Table 1 Main equipment and parameters

Module	Parameters
High-voltage power	24V input, $\le 1500V$ output
Spectrometer	Wavelength: 185-1000 nm, slit size: 10 μm
Control board	Communication via RS485
Peristaltic pump	Flow: 0 ~ 15 ml/L
Piston pump	Maximum Capacity: 5 ml, Accuracy: 0.002 ml, Number of channels: 12
Switching valve	Number of channels: 6, Number of states: 2

Hardware Design. Hardware components of the ASP-SCGD-OES system are organized by adopting an integrated sample handling principle, a critical feature that distinguishes it from conventional laboratory-bound SCGD setups.

As the core design of the system, sample injection and preparation subsystem consists of a programmable piston pump coupled to a multi-port switching valve, enabling fully automated on-site preparation and injection. The fluidic network is connected to reservoirs containing water samples for on-site analysis, a nitric acid buffer solution (pH 0.7, for sample acidification), nitric acid

(pH 1, for maintain the discharge), deionized water, standard solutions of target metal ions with gradient concentrations, a waste tank, a temporary storage tank, and a 4 mL quantitative sample loop.

The SCGD discharge unit, a component critical for atomization and excitation, was constructed based on our previously optimized design.^{10, 29} The liquid sample is delivered via a capillary tube (0.4 mm inner diameter, 0.8 mm outer diameter), acting as a solution cathode. A tungsten rod anode is positioned approximately 2.5 mm above the capillary tip. After applying a high DC voltage, a stable plasma is ignited at the solution-gas interface. The light emitted from the plasma is collected by a focusing lens and transmitted through an optical fiber to a spectrometer for dispersion and detection.

The key hardware components and their technical specifications are listed in Table 1. The entire system is housed in a compact enclosure (450 mm \times 350 mm \times 650 mm) with a total weight of 20 kg and an operational power consumption of less than 150 W, making it suitable for field deployment. The total cost of the system was kept to \$7,000.

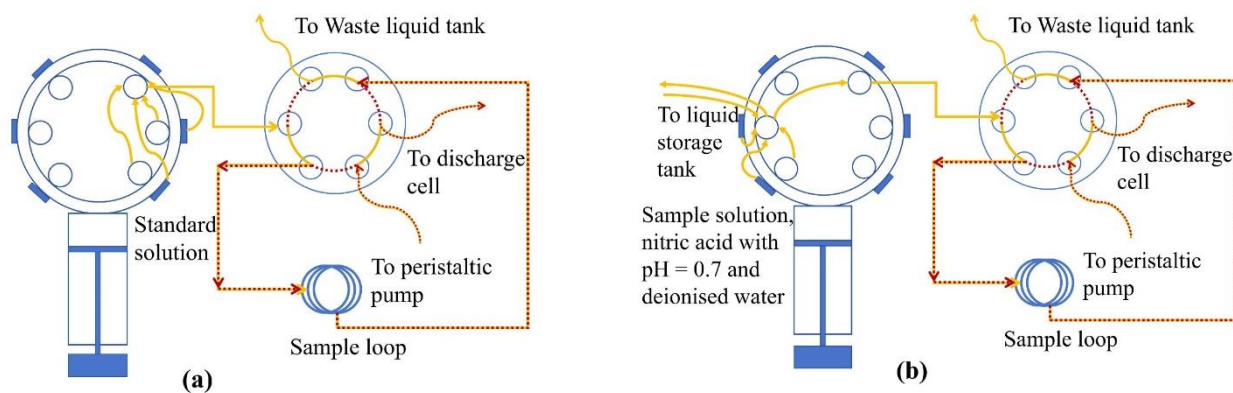


Fig. 3 Schematic diagram of the sample preparation and injection system. (a) Standard sample test state. (b) On-site sample preparation and the sample test state.

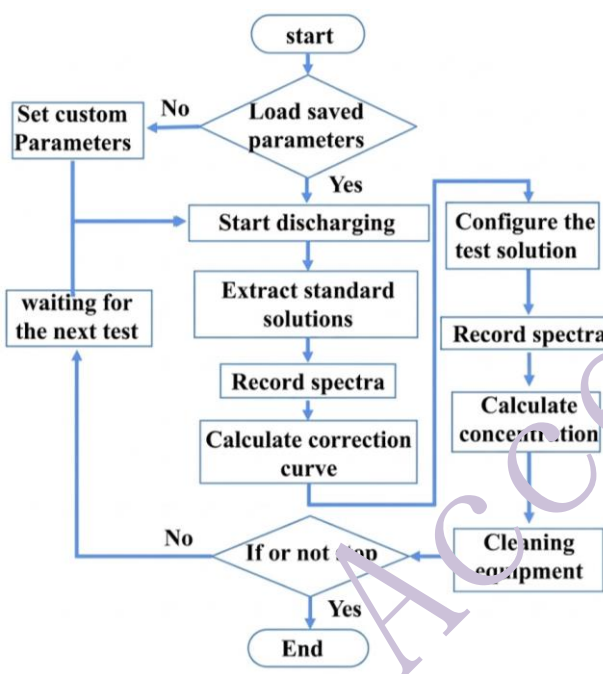


Fig. 4 The operational flow chart of the developed software.

Automated sample preparation workflow. The entire sample preparation and injection process for the instrument comprises four distinct states, and fluidic paths for the key states are given in detail in Fig. 3.

(1) System Priming State: The system initiates with a pre-test state, in which the switching valve directs the pH = 1 nitric acid to the discharge unit using a peristaltic pump to stabilize plasma.

(2) Standard-Sample Testing State: The piston pump aspirates predefined volumes of standard solutions at specified concentration gradients, Fig. 3(a), filling in the sample loop

(yellow solid line). The switching valve then redirects the flow to flush the standard solution from the loop to the discharge unit for subsequent calibration and analysis (red dotted line).

(3) On-site Sample Preparation State: After the calibration, environmental samples are prepared, Fig. 3(b). As illustrated in the piston pump aspirates a metered volume of on-site water, mixes it with a precise amount of the acid buffer in the storage tank to ensure consistent pH, and then transfers the homogenized mixture into the sample loop (yellow solid line).

(4) On-site Sample Testing State: Finally, the prepared sample is directed in the loop to the discharge unit for spectral analysis (red dotted line), completing the automated measurement cycle.

Software System Design. A dedicated software application was developed using C# on the .NET Framework to integrate control, sequencing, and analytical functions. The developed software communicates with the spectrometer via a USB interface and with the microcontroller board via RS485, creating a unified control platform.

The operational workflow of the software is depicted in Fig. 4. Upon launching, users can configure all measurement parameters, including discharge voltage, pump flow rates, and the spectrometer integration times for each targeted element, or load predefined parameter sets. Once initiated, the software automatically executes the following sequence:

(1) Initialization: The system is set to the pre-test state, the DC power supply is enabled, and the plasma is ignited and stabilized.

(2) Calibration: The software commands the hardware through the standard-sample testing sequence. It acquires spectra from each gradient standard solution, automatically identifies the characteristic emission lines for targeted metal elements, and constructs individual calibration curves.

(3) Sample Analysis: The software triggers the on-site sample preparation and testing sequence. It acquires raw spectra, applies calibration curves for targeted metal species, and calculates the corresponding concentrations of the analyzed metals.

(4) Data Logging: All raw spectra, calculated concentrations, and system metadata are automatically saved.

(5) System Maintenance: After the measurement and saving the data, the system flushes the entire fluidic path with deionized water to prevent cross-contamination and enters a low-power standby mode until the next scheduled measurement cycle.

RESULTS AND DISCUSSION

Optimization of Key Experimental Parameters. The analytical performance of the ASP-SCGD-OES metal monitoring system is significantly influenced by the chemical and operational conditions of the discharge process. To establish a compromise between the intensity of the spectral signal and plasma stability, since both are critical for reliable, long-term online monitoring, the effects of solution pH and discharge voltage were systematically investigated using standard Mg solutions.

The solution pH is a primary factor governing plasma characteristics and excitation efficiency. The respective emission intensity of 10 mg/L Mg, 10 mg/L Na, 10 mg/L K and 30 mg/L Ca solution is measured across a range of nitric acid concentrations (pH 0.8 to 2, $n=5$), Fig. 5, indicating a pronounced dependence of the emission intensity on acidity. At pH 2, the intensity is relatively low, but it steadily increases as the pH decreases which is consistent with previously reported observations of enhanced excitation efficiency in more acidic media. However, a drop in the signal intensity appears under strongly acidic conditions. At pH 0.8, frequent plasma quenching occurs, leading to a sharp decline in the signal intensity and unstable operation. An intermediate pH value of 0.9 is not reliable for continuous monitoring, as it occasionally suffers from discharge interruption over extended periods. This observed trend is broadly consistent with previous studies⁹, apart from the decrease in excitation intensity caused by plasma quenching. Consequently, a solution pH of 1.0 was selected for all subsequent experiments, as it provides a robust combination of the high signal intensity and sustained plasma stability.

The discharge voltage determines the energy input into the plasma, directly affecting analyte excitation. The relationship between the applied voltage (already accounting for the voltage drop across the ballast resistor) and the respective excitation intensities for 10 mg/L Mg, 10 mg/L Na, 10 mg/L K and 30 mg/L Ca solution at pH 1, Fig. 6(a), shows that the signal intensity increases with the applied discharge voltage due to the greater

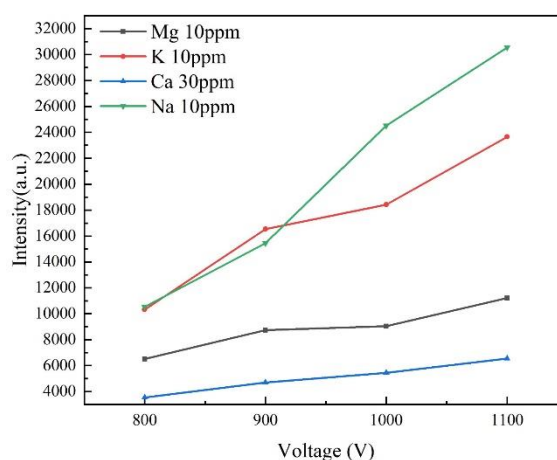


Fig. 5 Spectral line intensities obtained from nitric acid solutions containing 10 mg/L each of Na, K, and Mg, and 30 mg/L of Ca at different pH values.

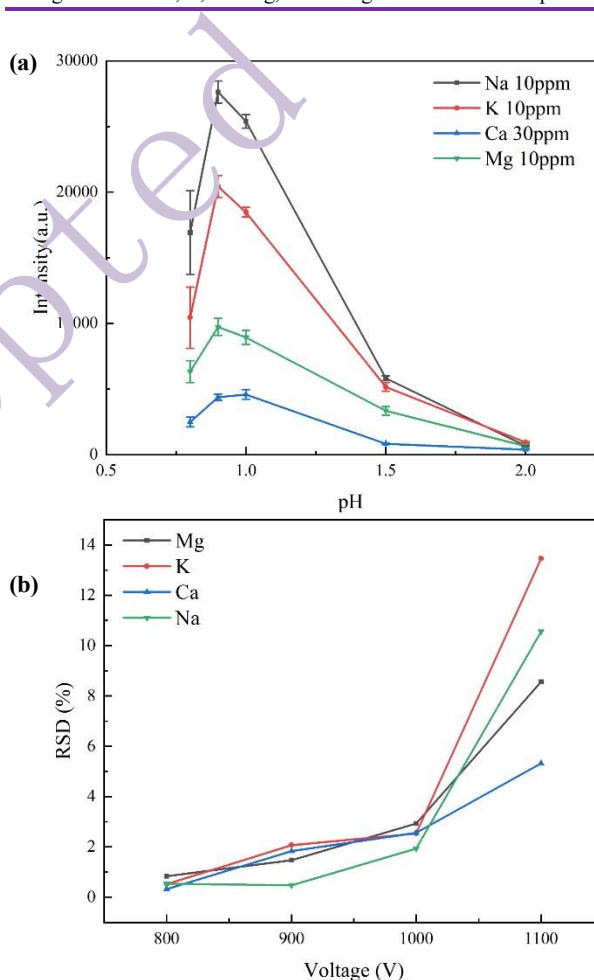


Fig. 6 Effect of discharge voltage on (a) spectral line intensities and (b) corresponding relative standard deviations (RSDs), obtained from nitric acid solutions containing 10 mg/L each of Na, K, and Mg, and 30 mg/L of Ca.

energy available for atomization and excitation. The variation in excitation intensity caused by the discharge voltage is broadly consistent with previous studies⁹. However, this gain in sensitivity

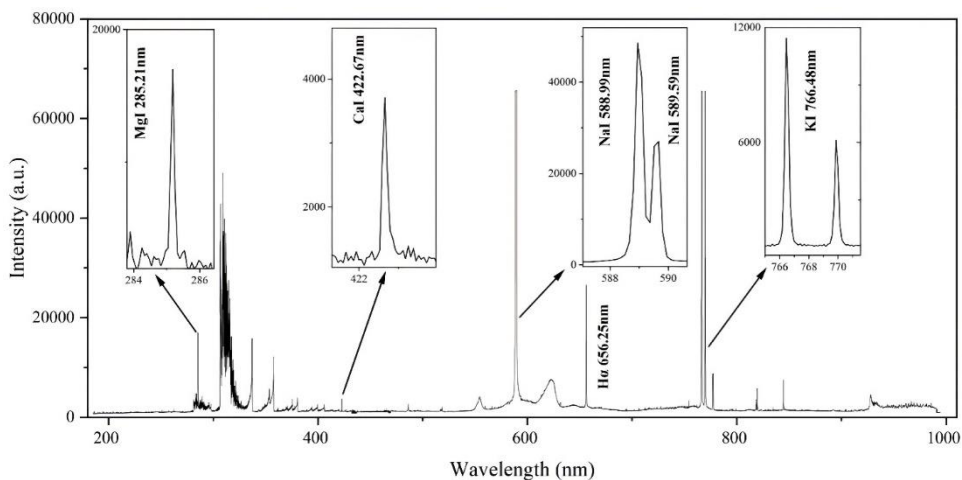


Fig. 7 The spectrum (integration time: 500 ms, except for Na and K, for which the integration time was 20 ms) of the riverine water sample showing characteristic Na, K, Ca, and Mg emissions.

Table 2 Comparison of the LODs of Na, K, Ca, and Mg for ASP-SCGD-OES, SCGD-OES, and ICP-OES systems

Element	LOD ($\mu\text{g/L}$)		
	ASP-SCGD-OES	SCGD-OES	ICP-OES
Na	0.12	0.14	7.1 ³²
K	1.1	4.1	0.33 ³³
Ca	280	110	1.9 ³⁴
Mg	26	55	1.51 ³³

leads to the scattering in the signal intensity, accompanying a concomitant increase in the relative standard deviation (RSD) (as shown in Figure 6(b), $n = 5$), and indicating greater signal fluctuation and degraded plasma stability at elevated discharge voltages. To prioritize analytical robustness for autonomous field operation, a discharge voltage of approximately 1000 V was chosen as the standard operating condition, offering a favorable balance between adequate sensitivity and operational stability.

Based on the above investigations, combined with the optimal solution flow rate and anode-cathode distance established in our previous work^{10,26}, the following parameters were applied without further modification for all performance evaluations: solution pH of 1.0, solution flow rate of 2 mL/min, and anode-cathode distance of 2.5 mm. The spectrometer integration times were tailored for each element to maximize the signal-to-noise ratio within the dynamic range of the detector (Na: 10 ms; Mg and K: 20 ms; Ca: 500 ms). A representative spectrum of a riverine water sample acquired under these optimized experimental conditions is presented in Fig. 7, clearly showing the characteristic emission lines of Na, K, Ca, and Mg. This observation confirms that the target cations can be simultaneously excited by the microplasma, producing distinct and well-resolved emission peaks without severe spectral overlap.

Limit of Detection (LOD). The LOD is a critical figure of merit for any analytical system. To evaluate whether the extended fluidic path of the integrated ASP-SCGD-OES monitoring system adversely affected intrinsic sensitivity, the LODs of Na, K, Ca, and Mg were determined under optimized operating conditions (discharge voltage: 1000 V). The LOD for each element was calculated based on Eq. (1):

$$LOD = 3 \times \sigma / S \quad (1)$$

Where σ is the standard deviation measured in a blank solution (nitric acid solution with a pH of 1), and S is the slope of the corresponding calibration curve.

The resulting LODs are summarized in Table 2, alongside literature values for conventional laboratory SCGD-OES systems and typically used ICP-OES. The LODs achieved by our online monitoring system are 0.12, 1.1, 280, and 26 $\mu\text{g/L}$ for Na, K, Ca, and Mg, respectively. While these values are comparable to, and in the case of Mg, superior to reported SCGD setups^{21,30}, they are higher than the best values obtained using specialized laboratory-scale SCGD configurations^{22, 31} and ICP-OES.³²⁻³⁴ These achievements can be primarily attributed to the use of a compact, low-resolution spectrometer in our current monitoring system, which is a necessary compromise between portability and field deployment. Nevertheless, employing a spectrometer with higher spectral resolution and optical throughput is expected to significantly suppress the background noise and improve the signal-to-noise ratio, thereby lowering the LODs of certain elements and potentially bringing the performance closer to that of ICP-OES.

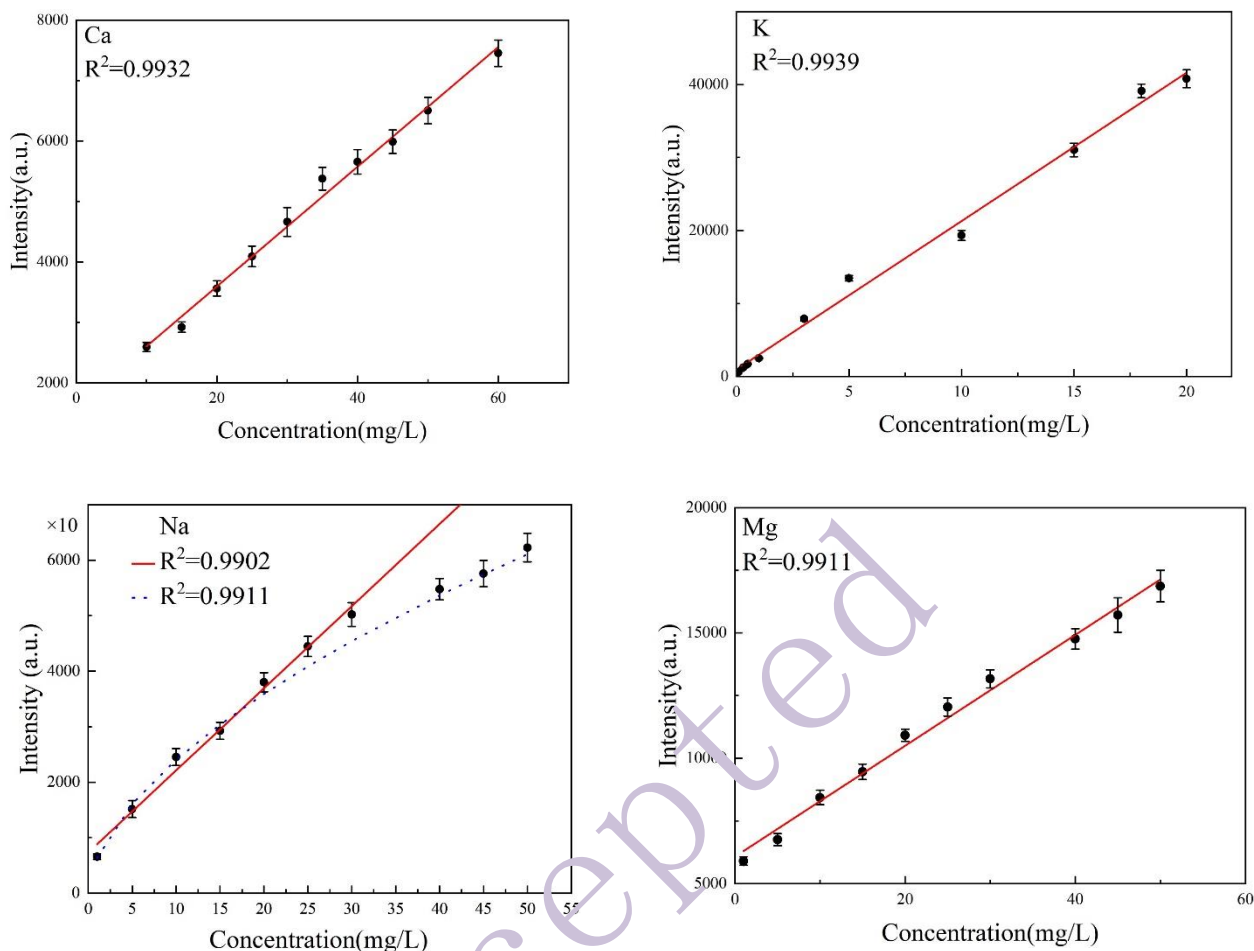


Fig. 8 ASP-SCGD-OES-derived calibration curves for Ca, K, Na, and Mg, for the concentration range corresponding to the content of these metals in riverine water samples for LOD calculations.

Quantitative Performance. For practical online monitoring of surface water, the quantitative accuracy at typical environmental concentrations (often in the ppm range) is more critical than ultralow LODs. Therefore, the quantitative measurement ability of the developed monitoring system was assessed using certified reference materials (CRMs, GBW(E)082051).

Firstly, the dynamic ranges for the ion concentrations of Na, K, Ca and Mg in typical river water were established. It should be noted that these tests were conducted in a laboratory setting, and calibration curves for each element were established using eight single-element standard solutions with varying concentrations. The dynamic ranges for each of the elements Na, K, Ca and Mg were 1–30 mg/L, 0.1–20 mg/L, 10–60 mg/L and 1–50 mg/L respectively ($n=10$). The emission intensities of Mg, K, and Ca exhibit a strong linear relationship with their concentrations across the tested ranges, Fig. 8. For Na, however, significant self-absorption occurs at higher concentrations, leading to a non-linear

response. This behavior is effectively modeled using the Scheibe-Lomakin function:

$$I_{Na} = a \cdot C_{Na}^b \quad (2)$$

Where I_{Na} is the intensity of the spectral peaks of Na, and C_{Na} is the concentration of Na ions. a and b are constants determined from fitting. The Scheibe-Lomakin function provides a reliable fit over the entire concentration range (blue dotted line in Fig. 8). At lower Na concentrations (< 35 mg/L), a linear fit is applicable; the integrated control software automatically selects the appropriate fitting model based on the obtained R^2 value, ensuring optimal quantitative accuracy.

Subsequently, the CRM sample (Na: 30 mg/L, Mg: 20 mg/L, K: 3 mg/L, Ca: 60 mg/L) was analyzed consecutively eight times ($n=8$), Fig. 9, demonstrating good accuracy and repeatability of the results. The mean relative errors (MREs) between the measured

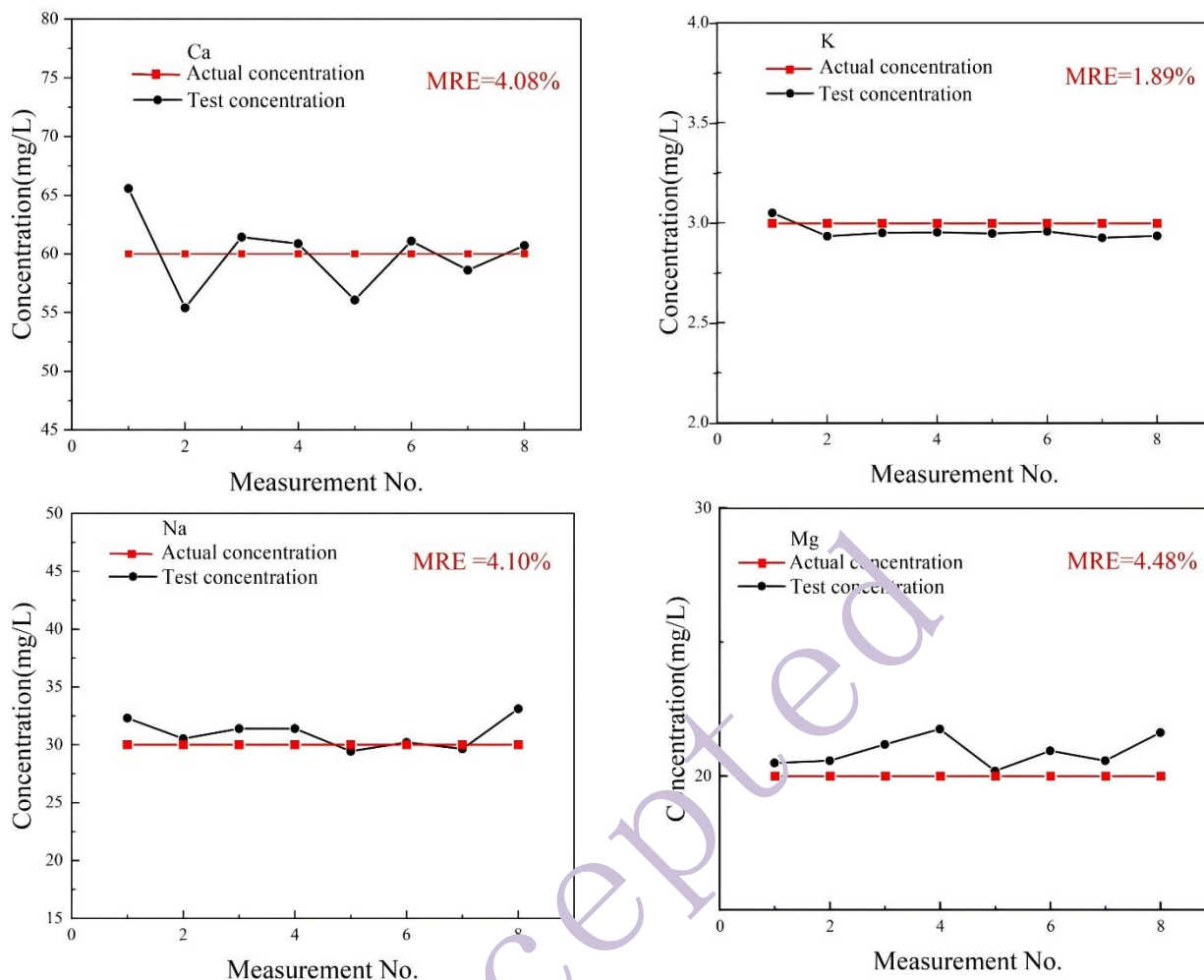


Fig. 9 Measurement results and errors of standard certified material water samples.

Table 3 Relative errors between the concentration (mg/L) determined using the developed ASP-SCGD-OES system and traditional ICP-OES analysis.

Element	Sample 1			Sample 2			Sample 3		
	ASP- SCGD-OES	ICP-OES	Relative error (%)	ASP- SCGD-OES	ICP-OES	Relative error (%)	ASP- SCGD-OES	ICP-OES	Relative error (%)
K	5.83	5.52	5.74	5.72	5.69	0.55	5.60	5.74	-2.44
Na	26.65	27.63	-3.53	29.29	28.33	3.41	34.67	35.53	-2.41
Ca	53.07	52.99	0.15	53.39	53.74	-0.63	66.51	67.23	-1.06
Mg	11.15	11.93	-6.47	12.42	12.01	3.46	14.80	15.57	-4.93

and certified values are 4.1%, 4.5%, 1.9%, and 4.1% for Na, Mg, K, and Ca, respectively. These errors fall within acceptable limits for environmental analysis, confirming that the ASP-SCGD-OES monitoring system, calibrated with a simple four-point curve, exhibits an excellent quantitative performance for major cations in riverine water.

Online analytical performance. The ultimate validation of the system's performance was conducted as a continuous, 7-day field deployment study at the Jinjia River in Chongqing (106.67°E, 29.63°N). The monitoring system operated autonomously,

performing hourly measurements, including automated recalibration cycles with standard solutions before each sample analysis. Throughout these 7 days, only routine replenishment of reagents was performed, requiring no maintenance or manual intervention on the core system.

The concentration trends for all four targeted elements over the testing period are shown in Fig. 10, demonstrating the system's stability and ability to track dynamic changes in water quality. Three water samples were collected at different times and subjected to reference analysis by ICP-OES for a rigorous

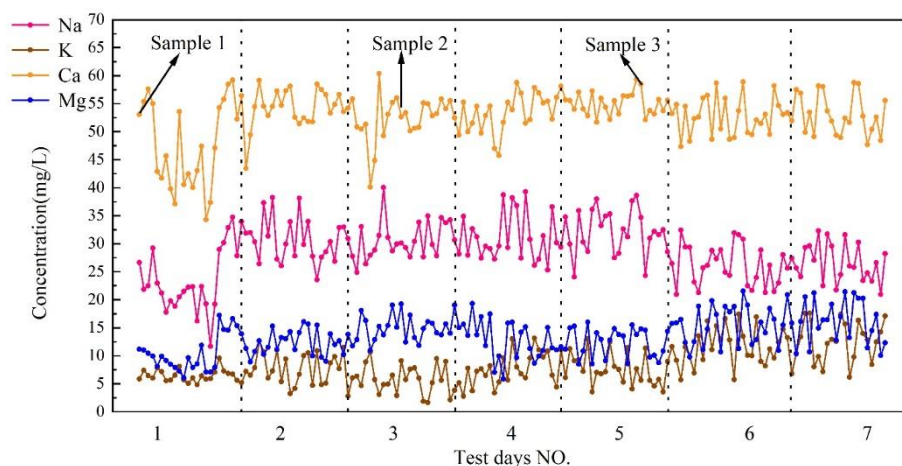


Fig. 10 Continuous monitoring of the concentration of major metals in the Jinjia River in Chongqing (106.67°E, 29.63°N).

Table 4. Comparison of the proposed ASP-SCGD-OES system with recently reported analytical technologies for on-site/online monitoring of metal ions in water

Analytical Technology	Target Ions	Main Consumables	Sample Pretreatment & Online Capability	Main Bottlenecks for Field Deployment	Ref.
Portable Microplasma OES	Trace metals	Compressed Argon & Reagents	Online flow injection & digestion	Strictly limited by the capacity of heavy gas cylinders	35
Microfluidic Electrochemical (ASV)	Heavy metals	Specific electrolytes	Microfluidic automated handling	Severe electrode fouling in raw water; requires frequent electrode regeneration	36
Continuous Flow Portable XRF	Heavy metals	None	Continuous flow cell pumping	The sample preparation time is relatively long (15 minutes); radiation safety concerns	37
Conventional SCGD-OES	Na, K, Ca, Mg, etc.	None (Ambient air)	Strictly manual acidification (pH=1.0)	Absolutely requires manual intervention;	38
Proposed ASP-SCGD-OES	Na, K, Ca, Mg	Nitric acid buffer (pH=0.7)	Fully automated buffering & mixing	Demonstrated 168-h highly robust autonomous operation without any carrier gas	This work

accuracy test. The results from the ASP-SCGD-OES monitoring system, Table 3, show excellent agreement with the reference method, and the relative errors for all the elements and across all samples fall within 5.7%, with a minimum error of just 0.2% for Ca.

This successful field trial confirms several key advantages of the developed monitoring system: 1) Robustness: It operates effectively under variable field conditions, requiring minimal human involvement. 2) Accuracy: Its measurement results are consistent with a standard laboratory technique (ICP-OES). This confirms that the ASP-SCGD-OES monitoring systems maintains its measurement integrity throughout a typical maintenance cycle, making it a viable solution for the long-term distant water quality monitoring. It is worth noting that, as the concentrations of these four target ions in actual river water (< 100 ppm) are not particularly high, the interactions between them are very weak; consequently, in practical monitoring, these interactions are not taken into account, a finding that is consistent with previous research¹⁷.

Comparison with recent on-site analytical technologies. To comprehensively evaluate the engineering and practical merits of the proposed system, we benchmarked it against recently reported advanced technologies dedicated to the on-site and online monitoring of metal ions in water, as summarized in Table 4. Recent developments in portable microplasma sources³⁵ exhibit excellent sensitivity but still impose a severe logistical burden for continuous field deployment due to their reliance on compressed argon cylinders. Alternative gas-free approaches also face inherent bottlenecks in complex natural water matrices: automated microfluidic electrochemical sensors (e.g., ASV) are highly susceptible to electrode fouling and demand frequent regeneration³⁶, while continuous-flow portable X-ray fluorescence (pXRF) systems struggle with extremely poor sensitivity for light major cations like Na and Mg³⁷. Furthermore, conventional SCGD-OES systems, though gas-free, remain strictly tethered to laboratory environments because they completely lack automated matrix standardization capabilities³⁸.

In stark contrast, the proposed ASP-SCGD-OES system successfully circumvents these critical limitations. By thoroughly

automating the sample pretreatment (pH=0.7 buffering) and eliminating the need for carrier gases, our system enables fully automated, continuous online monitoring of common metal ions in river water. This enables an unprecedented 168 hours of continuous, unattended operation, marking a step forward for the robust field deployment of microplasma spectrometry.

CONCLUSION

In this study, a fully automated sample preparation solution cathode glow discharge optical emission spectrometry (ASP-SCGD-OES) system was successfully developed, fundamentally breaking the bottleneck of manual offline pretreatment that has long restricted the field deployment of microplasma sources. By integrating peristaltic pump-driven continuous flow sample introduction with piston pump-mediated discrete injection, the ASP module automatically standardizes the raw environmental water with nitric acid (pH = 0.7) and performs system calibration. Furthermore, by eliminating the reliance on carrier gases, lowering the energy consumption required for field deployment, and minimizing the need for continuous manual intervention, this automated architecture drastically reduces the overall operational and maintenance costs, offering a highly economical platform for long-term environmental monitoring.

The analytical performance of the integrated system was rigorously validated. The system achieves detection limits of 0.12, 1.1, 280 and 26 µg/L for Na, K, Ca and Mg respectively, alongside excellent linearity in typical concentration ranges in surface water ($R^2 > 0.99$). Its quantitative reliability was confidently verified through both Certified Reference Material analysis and cross-validation against laboratory ICP-OES. Most significantly, the system demonstrated operational autonomy during a 168-hour continuous, unattended field deployment for the monitoring of major cations (Na, K, Ca, and Mg) in river water.

Furthermore, the programmable and modular nature of the ASP fluidic network provides a highly scalable foundation for future analytical expansions. By flexibly incorporating online preconcentration techniques (e.g., micro-solid-phase extraction) or chemical vapor generation (CVG) protocols into the current automated workflow, the analytical capability of this portable platform can be readily extended from major cations to the continuous, on-site monitoring of toxic heavy metals. Thus, by bridging the gap between laboratory-grade spectral analysis and robust, carrier-gas-free automation, this work paves the way for comprehensive, next-generation environmental monitoring networks. Nevertheless, it must be acknowledged that a comprehensive assessment of significant matrix effects is beyond the scope of this preliminary study, as the samples analysed in this paper were river water, for which matrix effects are not significant, as demonstrated by cross-validation with ICP-

OES. The systematic investigation and resolution of these complex interferences will be highly prioritized in our future work to further expand the instrument's application boundaries.

AUTHOR INFORMATION



Peichao Zheng received his Ph.D. from the Anhui Institute of Optics and Mechanics, Chinese Academy of Sciences, in 2009, and has conducted visiting research at Indiana University Bloomington in the United States. His research focuses on the development of novel optoelectronic sensing technologies and devices. Addressing the need for rapid component measurement in environmental monitoring, agriculture, and industrial process control, he employs techniques such as emission spectroscopy, absorption spectroscopy, and fluorescence spectroscopy to investigate new detection mechanisms, develop key components, and design metrological algorithms and sensing devices. He has published over 100 high-impact papers in academic journals both domestically and internationally.

Corresponding Author

*P. C. Zheng

Email address: zhengpc@cqupt.edu.cn

*J. M. Wang

Email address: wangjm@cqupt.edu.cn

Notes

The authors declare no competing financial interest.

ACKNOWLEDGMENTS

The authors would like to express their gratitude to EditSprings (<https://www.editsprings.com>) for the expert linguistic services provided.

The authors acknowledge the use of artificial intelligence (AI) tools strictly for English language polishing, and take full responsibility for the final content of this manuscript.

This work was supported by National Natural Science Foundation of China (62575044), Science and Technology Research Program of Chongqing Municipal Education Commission (KJZD-M202200602), Natural Science Funding of Chongqing (CSTB2024NSCQ-LZX0078), Chongqing

REFERENCES

1. M. D. Sui, Y. S. Fan, L. L. Jiang, Y. Y. Xue, J. Zhou, and S. L. Zhong, *Spectrochim. Acta B*, 2021, **180**, 106201-106211. <https://doi.org/10.1016/j.sab.2021.106201>
2. M. Gao, J. H. Shi, Q. Li, and Z. Wang, *Microchem. J.*, 2025, **213**, 113695-113700. <https://doi.org/10.1016/j.microc.2025.113695>
3. H. W. Li, W. C. Zu, F. K. Liu, Y. Wang, Y. Yang, X. T. Yang, and C. Liu, *Spectrochim. Acta B*, 2019, **152**, 25-29. <https://doi.org/10.1016/j.sab.2018.12.004>
4. J. Yu, Z. C. Zhang, Q. F. Lu, D. X. Sun, S. W. Zhu, X. M. Zhang, X. Wang, and W. Yang, *J. Anal. Methods Chem.*, 2017, **2017**, 7105831. <https://doi.org/10.1155/2017/7105831>
5. P. Punia, M. K. Bharti, R. Dhar, P. Thakur, and A. Thakur, *ChemBioEng Rev.*, 2022, **9**, 351-369. <https://doi.org/10.1002/cben.202100053>
6. Q. Ding, C. Li, H. J. Wang, C. L. Xu, and H. Kuang, *Chem. Commun.*, 2021, **57**, 7215-7231. <https://doi.org/10.1039/D1CC00983D>
7. M. Wellinger, J. Wochele, S. M. A. Biollaz, and C. Ludwig, *Waste Manage.*, 2012, **32**, 1843-1852. <https://doi.org/10.1016/j.wasman.2012.05.015>
8. T. Cserfalvi, P. Mezei, and P. Apai, *J. Phys. D Appl. Phys.*, 1993, **26**, 2184-2188. <https://doi.org/10.1088/0022-3727/26/12/015>
9. M. R. Webb, F. J. Andrade, G. Gamez, R. McCrindle, and G. M. Hieftje, *J. Anal. At. Spectrom.*, 2005, **20**, 1218-1225. <https://doi.org/10.1039/b503961d>
10. J. M. Wang, W. Li, P. C. Zheng, B. Li, B. Y. Zhang, L. L. Guo, H. W. Tian, and D. M. Dong, *J. Anal. At. Spectrom.*, 2025, **40**, 346-353. <https://doi.org/10.1039/d4ja00335g>
11. R. Manjusha, M. A. Reddy, R. Shekhar, and S. Jaikumar, *J. Anal. At. Spectrom.*, 2013, **28**, 1932-1939. <https://doi.org/10.1039/c3ja50202c>
12. R. Shekhar, *Talanta*, 2012, **93**, 32-36. <https://doi.org/10.1016/j.talanta.2012.02.004>
13. K. Greda, P. Jamróz, and P. Pohl, *Talanta*, 2013, **108**, 74-82. <https://doi.org/10.1016/j.talanta.2013.02.049>
14. Q. F. Lu, F. F. Feng, J. Yu, L. Yin, Y. J. Kang, H. Luo, D. X. Sun, and W. Yang, *Microchem. J.*, 2020, **152**, 104308-104316. <https://doi.org/10.1016/j.microc.2019.104308>
15. H. B. Khanh, N. L. Duy, N. A. Tien, and N. H. D. Khang, *Spectrochim. Acta B*, 2024, **219**, 107000. <https://doi.org/10.1016/j.sab.2024.107000>
16. J. M. Wang, Y. X. He, S. Shata, M. J. Shultz, H. I. A. Qazi, M. N. Wu, N. T. Yan, G. X. Fei, and P. C. Zheng, *Anal. Lett.*, 2023, **56**, 2937-2950. <https://doi.org/10.1080/00032719.2023.2189733>
17. J. Yu, X. M. Zhang, Q. F. Lu, L. Yin, F. F. Feng, H. Luo, and Y. J. Kang, *Acs. Omega.*, 2020, **5**, 19541-19547. <https://doi.org/10.1021/acsomega.0c01906>
18. L. Bencs, N. Laczai, P. Mezei, and T. Cserfalvi, *Spectrochim. Acta B*, 2015, **107**, 139-145. <https://doi.org/10.1016/j.sab.2015.03.003>
19. P. C. Zheng, Y. M. Gong, J. M. Wang, and X. B. Zeng, *Anal. Lett.*, 2017, **50**, 1512-1520. <https://doi.org/10.1080/00032719.2016.1233243>
20. M. Gorska, J. Weiss, and P. Pohl, *Anal. Methods-Uk*, 2023, **15**, 1775-1789. <https://doi.org/10.1039/d3ay00092c>
21. X. Wang, X. Liu, L. L. Jin, Z. L. Zhu, J. H. Dong, P. J. Xing, L. J. Chen, Y. H. Geng, J. W. Zhang, H. Tong, H. T. Zheng, M. Zhang, and S. H. Hu, *J. Anal. At. Spectrom.*, 2024, **39**, 3198-3206. <https://doi.org/10.1039/d4ja00264d>
22. J. Yu, X. M. Zhang, Q. F. Lu, X. Wang, D. X. Sun, Y. Q. Wang, and W. Yang, *Talanta*, 2017, **175**, 150-157. <https://doi.org/10.1016/j.talanta.2017.07.040>
23. J. Z. Liu, J. H. Dong, S. R. Han, J. W. Zhang, X. Liu, H. T. Zheng, and Z. L. Zhu, *J. Anal. At. Spectrom.*, 2024, **39**, 1343-1352. <https://doi.org/10.1039/d4ja00035h>
24. W. C. Zu, Y. Wang, X. T. Yang, and C. Liu, *Talanta*, 2017, **173**, 88-93. <https://doi.org/10.1016/j.talanta.2017.05.073>
25. X. X. Peng, X. H. Guo, F. Ge, and Z. Wang, *J. Anal. At. Spectrom.*, 2019, **34**, 394-400. <https://doi.org/10.1039/c8ja00369f>
26. P. C. Zheng, Q. H. H. X. Zhang, J. M. Wang, Y. Yang, Y. X. He, M. N. Wu, H. W. Tian, D. M. Dong, X. F. Mao, and C. H. Lai, *Anal. Lett.*, 2022, **55**, 2273-2285. <https://doi.org/10.1080/00032719.2022.2053146>
27. J.-H. Dong, C. Yang, H.-Q. Ding, P.-J. Xing, F.-Y. Zhou, H. Tian, X. Liu, H. T. Zheng, S.-H. Hu, and Z.-L. Zhu, *Anal. Chem.*, 2021, **93**, 13351-13359. <https://doi.org/10.1021/acs.analchem.1c03133>
28. J. Dong, C. Yang, D. He, H. Zheng, S. Hu, and Z. Zhu, *Atom. Spectrosc.*, 2020, **41**, 57-63. <https://doi.org/10.46770/AS.2020.02.002>
29. P. C. Zheng, J. T. Zhou, J. M. Wang, J. L. Liu, W. Li, B. Li, L. B. Guo, H. W. Tian, and D. M. Dong, *J. Anal. At. Spectrom.*, 2025, **40**, 1284-1296. <https://doi.org/10.1039/d4ja00421c>
30. P. Pohl, P. Jamroz, K. Greda, M. Gorska, A. Dzimitrowicz, M. Welna, and A. Szymczycha-Madeja, *Anal. Chim. Acta*, 2021, **1169**, 338399. <https://doi.org/10.1016/j.aca.2021.338399>
31. C. Yang, L. Wang, Z. L. Zhu, L. L. Jin, H. T. Zheng, N. S. Belshaw, and S. H. Hu, *Talanta*, 2016, **155**, 314-320. <https://doi.org/10.1016/j.talanta.2016.04.060>
32. M. T. Lisboa, C. D. Clasen, D. C. de S. Vellar, E. Q. Oreste, T. D. Saint-Pierre, A. S. Ribeiro, and M. A. Vieira, *J. Brazil. Chem. Soc.*, 2014, **25**, 143-151. <https://doi.org/10.5935/0103-5053.20130280>
33. M. J. B. de Souza, M. C. Barciela-Alonso, M. Aboal-Somoza, and P. Bermejo-Barrera, *Braz. J. Anal. Chem.*, 2022, **9**, 49-61. <https://doi.org/10.30744/brjac.2179-3425.AR-87-2021>
34. J. Naozuka, E. C. Vieira, A. N. Nascimento, and P. V. Oliveira, *Food Chem.*, 2011, **124**, 1667-1672. <https://doi.org/10.1016/j.foodchem.2010.07.051>
35. J.-Y. Cai, X. Zhang, Y.-J. Wei, S. Chen, Y.-L. Yu, and J.-H. Wang, *Anal. Chem.*, 2024, **96**, 3733-3738. <https://doi.org/10.1021/acs.analchem.3c05330>
36. S. S. Ma, W. Zhao, Q. Zhang, K. Y. Zhang, C. Liang, D. K. Wang, X. T. Liu, and X. Zhan, *J. Hazard. Mater.*, 2023, **448**, 130923. <https://doi.org/10.1016/j.jhazmat.2023.130923>
37. T. E. Tiihonen, T. J. Nissinen, P. A. Turhanen, J. J. Vepsäläinen, J. Riikonen, and V.-P. Lehto, *Anal. Chem.*, 2022, **94**, 11739-11744. <https://doi.org/10.1021/acs.analchem.2c01490>
38. J. Yu, X. M. Zhang, Q. F. Lu, L. Yin, F. F. Feng, H. Luo, and Y. J. Kang, *Acs Omega*, 2020, **5**, 19541-19547. <https://doi.org/10.1021/acsomega.0c01906>

Accepted